Audio Engineering Society

Convention Paper 8888

Presented at the 134th Convention

2013 May 4–7 Rome, Italy

Digital Filter for Modeling Air Absorption in Real Time

CARLO PETRUZZELLIS, UMBERTO ZANGHIERI

ZP Engineering srl, Rome, 00131, Italy

ABSTRACT

Sound atmospheric attenuation is a relevant aspect of realistic space modeling in 3D audio simulation systems. A digital filter has been developed on commercial DSP processors to match air absorption curves. This paper focuses on the algorithm implementation of a digital filter with continuous roll-off control, to simulate high frequency damping of audio signals in various atmospheric conditions, along with rules to allow a precise approximation of the behavior described by analytical formulas.

1. INTRODUCTION

In 3D audio systems and in sound space modeling, simulation of high frequency audio damping in different atmospheric conditions allows realistic recreation of virtual environments. Analytical expressions modeling air absorption are available in [1] and [6], but are too complex for a useful real-time implementation. Previous works have focused on the use of digital filters, with matching obtained using classical filter design techniques [3]. The present work deploys a modified first-order digital low pass filter that offers a continuous control of roll-off in the frequency domain with a gentler slope than the usual 6dB/octave obtained with a classical first-order low pass filter. Two of these filters can be cascaded, and coefficients are derived from tabulated data, to model the response described in literature and allow direct control with a parameter representing the virtual sound source distance. Therefore, the goal of the present work is to describe an algorithm that allows defining environmental parameters independently from virtual source distance. The source distance has been restricted to a range of 10 to 70 meters, as this is the region with perceptual relevance for sound space modeling.

2. AIR ABSORPTION

When sound propagates in free air, it is attenuated in a frequency-dependent way, due to relaxation processes associated with the discrete internal vibrations of oxygen and nitrogen molecules [5]. Attenuation caused by air absorption is a function of temperature, relative humidity, atmospheric pressure and frequency, and has been analyzed and modeled extensively [1] [2] [4] [6] [7] [8]. As an example, using the formula available in [1], the effect of air absorption is shown in Figure 1, at a temperature of 20°C and relative humidity of 20%. It can be seen that as distance increases, high-frequency roll-off increases accordingly.

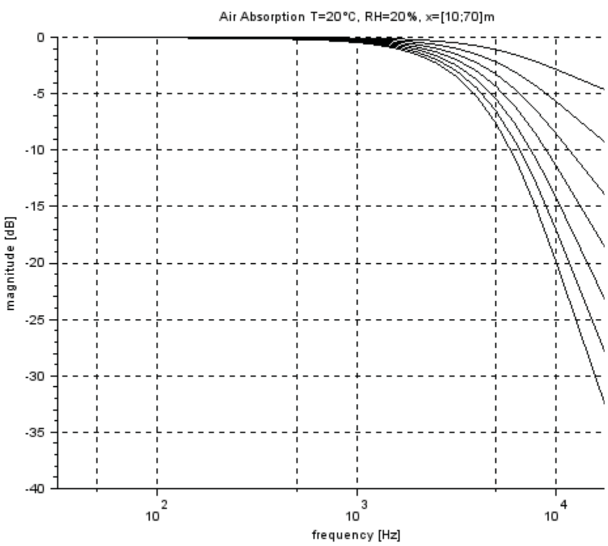

Figure 1: Air absorption filtering effect at 20°C and 20% RH; propagation distances vary from 10 to 70 meters in 10-meter steps

Air absorption attenuation values have been tabulated in literature for several values of temperature, relative humidity and propagation distances [1], and successive data inspection reveals that a way to model the variable high-frequency roll-off occurring mainly as a function of propagation distance is needed. A total of 24 different curves have been analyzed, with the following parameter variations:

- Temperature: from -20°C to 40°C in 20°C steps
- Relative humidity: from 10 % to 100% in 6 steps

3. SIMULATED ABSORPTION FILTER

Starting from a normalized first-order low pass filter topology [9] [10], a novel first-order filter has been derived with independent roll-off control that monotonically morphs filter behavior from Low-Pass to All-Pass. In the transfer function described in Eq. 1, coefficient *a* determines the frequency relative to the curve knee, while coefficient *b* affects the filter roll-off, so that:

- $b = 1 \rightarrow$ Low Pass Filter (6 dB/octave slope)
- $b = 0 \rightarrow$ All Pass Filter

For values of *b* less than 1, the algorithm is able to provide a slope with steepness lower than 6dB/octave. It will be referred in the text as SA (Simulated Absorption) filter.

$$H(z) = \frac{(a+b-1)+(1-b)z^{-1}}{1-(1-a)z^{-1}} \quad (1)$$

3.1. FILTER PROPERTIES

Coefficient *b* has a symmetric effect relative to a central point fixed in (1 – *a*/2); this value corresponds to the steepest frequency roll-off. Therefore, coefficient *b* values in the range [0; (1 - *a*/2)] result in the same effect of values in the range [(1 - *a*/2); (2 – *a*)]. These values delimit the useful range of *b* to obtain a variable slope frequency response. This property defines that a Low-Pass filter is obtained with *b* = (1 – *a*), as well as with *b* = 1. To better analyze the filter properties, the frequency responses obtained by varying one coefficient only have been plotted, while maintaining the other coefficient fixed. The evolution of frequency response of a SA filter, with coefficient *a* varying in range [0.01; 0.81] and coefficient *b* fixed at value 1 (LPF mode), is shown in the figure 2. For values of coefficient *a* larger than 0.81, the corner frequency remains fixed at a frequency of 0,5**SR*, whereas for values inside the [0.01; 0.81] range, the corner frequency varies from 0.014**SR* to 0.5*SR. Corner frequency values of the SA filter with incremental variations of coefficient *a* with a 0.05 step, are reported in Table 1.

a	freq [Hz]	*a*	freq [Hz]	*a*	freq [Hz]
0,01	70,38	0,31	3190,62	0,61	8774,19
0,06	516,13	0,36	3847,5	0,66	10392,96
0,11	958,34	0,41	4598,24	0,71	12574,78
0,16	1478,01	0,46	5419,35	0,76	15906,16
0,21	1994,13	0,51	6357,77	0,81	24000
0,26	2580,65	0,56	7460,41		

Table 1: Corner frequencies of SA filter with values of coefficients *a* in range [0,01; 0,81] and value of *b* fixed at 1 (LP filter), at 48 kHz sample rate

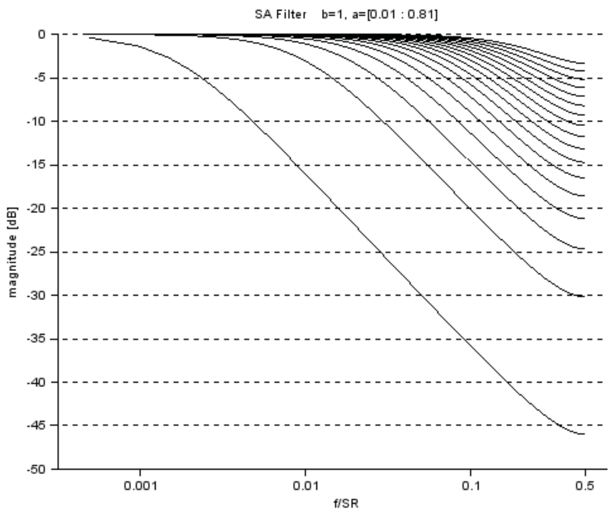

Figure 2: 1st order SA filter frequency response with $b = 1$ and $a = [0.01; 0.81]$.

The frequency response of a SA filter, with coefficient b values in the range [0; 0.94] and with coefficient a fixed at value 0.12 (corner frequency = 958.34 Hz), is shown in Figure 3. Due to the symmetric property of coefficient b, maximum slope of the SA filter, is obtained with $b = 0.94$, whereas a 6dB/octave slope is obtained with $b = 0.88$. For these values of coefficients ($a = 0.12$, $b = 0.94$), the roll-off frequency attenuation becomes -3.1 dB. Therefore, it can be shown that the maximum slope achievable with the SA first-order filter*,* corresponds to a roll-off frequency attenuation increase of only 0.1 dB compared to the usual Low-Pass filter (bold line in Figure 3).

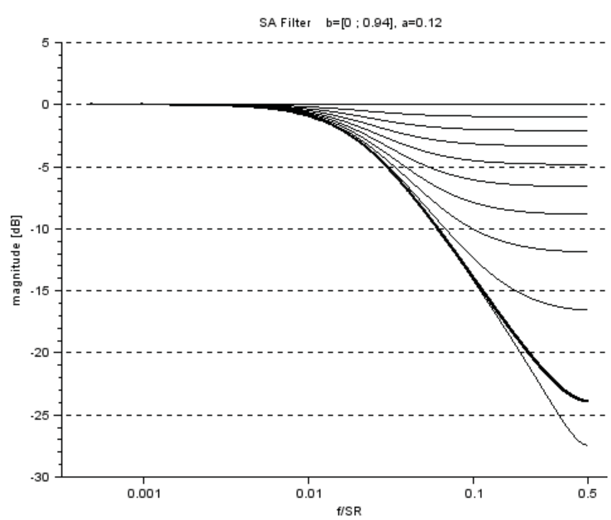

Figure 3: 1st order SA filter frequency response with $a = 0.12$ and $b = [0; 0.94]$.

In the actual implementation of a sound space modeling system, a cascade of two first-order SA filters has been used. This choice offers different slope and corner frequency combinations, allowing to precisely match the 24 absorption curves previously analyzed. Using the same (a, b) value pairs, the transfer function roll-off has doubled compared to the frequency response plots shown in fig. 2 and fig. 3.

The cascade of two SA filters is particularly suitable to simulate air absorption at low temperatures (lower than 0 °C). Therefore, as shown in figure 4 where temperature is fixed at 0°C and relative humidity is fixed at 10%, air absorption curves derived from analytical formulas [1] have two knees at different frequencies. Combining different value pairs of the filter coefficients, separately for each SA filter, it is possible to match these curves. Therefore, the shown structure is useful to match non-strictly decreasing functions, where slope and inflection point vary with source distance. On the other hand, above 0°C, the frequency response becomes a strictly decreasing function, as in figure 1; it is possible to achieve the desired curve roll-off by using the same value for coefficient a on both filters, related to the corner frequency, and combining different coefficient b values on the two SA filters. For temperatures above 0 °C, usage of first-order IIR filters, as described in [3], gives a similar frequency response.

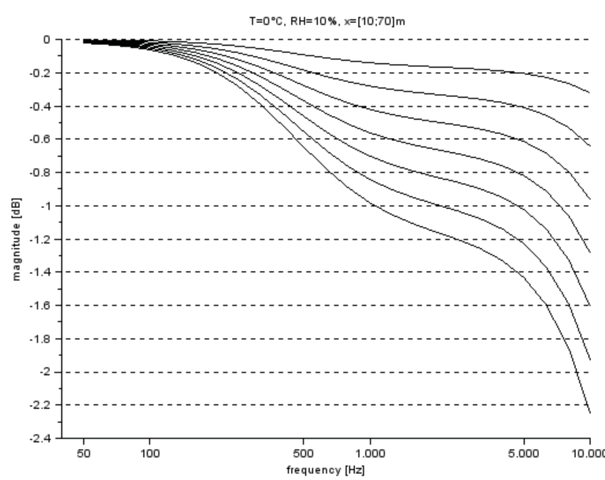

Figure 4: Air absorption curve for T = 0°C, RH = 10% and distance $x = [10:70]$ meters.

3.2. COMPUTATION OF COEFFICIENTS

In a cascade of two SA filters, by varying coefficients $a1$, $a2$ and $b1$, $b2$, the atmospheric absorption as a function of propagation distance x [m] and frequency f [Hz] has been modeled at various temperature and relative humidity values. For any pair of temperature (T) and relative humidity (RH) values, as a first step, $a1$ and $a2$ values are derived by matching corner frequencies. Then, $b1$ and $b2$ values are derived from heuristic formulas, derived experimentally and described in equations 2 and 3.

$$b_1(x)=(a_1+\frac{0,1}{a_2})\,0,1\,\frac{a_2}{K_1}x \qquad (2)$$

$$b_2(x)=(a_1+\frac{0,22}{a_2})\,0,1\,\frac{(1-a_1)}{K_2}x \qquad (3)$$

where x is the instantaneous virtual source distance from the listener, and $K1$, $K2$ are constant values that depend on temperature and relative humidity values selected for the atmospheric scenario to be simulated.

4. CURVE MODELING

In the actual implementation of a sound space modeling system, the source distance has been restricted to a range of 10 to 70 meters, as this is the region with highest perceptual relevance. For values of distance shorter than 10 meters, atmospheric attenuation is not perceptible by human ear because its value is on the order of 0.1 dB and can be approximated with an All Pass filter. A table of 24 different cases has been derived as described above, by varying temperature in the range of -20°C to 40 °C, and relative humidity in the range of 10% to 100%. As an example of results achieved, in Figure 5 the solid lines represent the atmospheric attenuation curve at a temperature of 0°C and relative humidity of 10% as in [1], whereas the dot lines represent the frequency response obtained from the cascade of two SA filters with pre-computed pairs of coefficients ($a1$, $b1$) and ($a2$, $b2$).

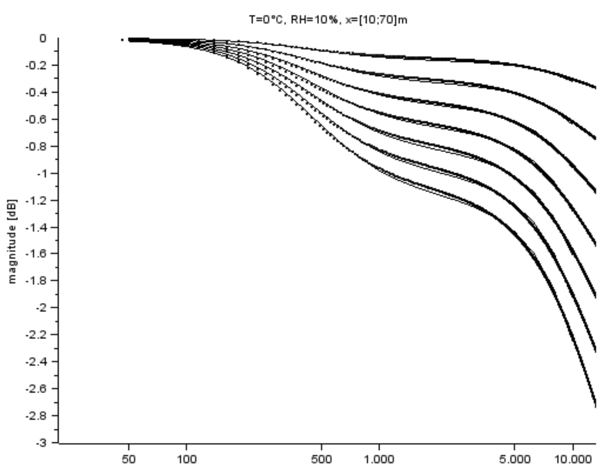

Figure 5: Matching curves between frequency response of two SA filters and air absorption curves for T = 0°C, RH = 10% and distance x = [10:70] meters

It has been verified that in the frequency range considered in [1], from 10 to 10000 Hz, curve matching is very close, and the maximum error is lower than 0.1 dB, as represented in Figure 6. Tables 2 and 3 list the values of coefficients a and b calculated for each filter that model atmospheric attenuation at low temperatures (-20°C and 0°C), in six cases of relative humidity (10%, 20%, 40%, 60%, 80%, 100%) and in seven cases of propagation distances (from 10 to 70 meters). For atmospheric conditions at high temperatures (20°C and 40°C), air absorption curves have no inflection point, and their frequency responses are strictly decreasing. In this case, the curve matching method uses same coefficient values for both SA filters, so that their frequency responses are summed. To allow a fine tuning of the roll-off, it is necessary to use different values for coefficients $b1$ and $b2$, while maintaining $a1 = a2$.

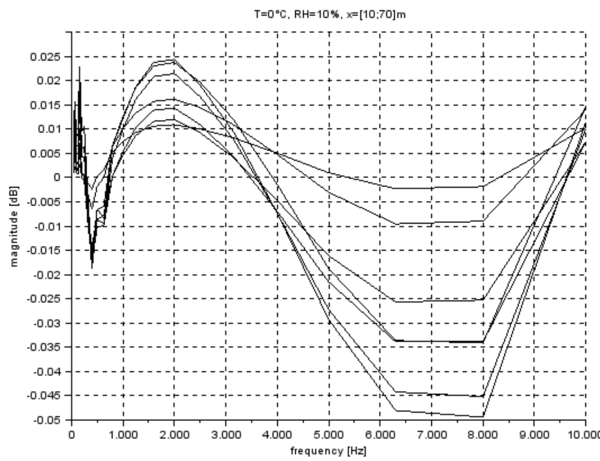

Figure 6. Matching error evaluated between air absorption curves and a cascade of two SA filters for propagation distances [10:70] meters.

5. CONCLUSIONS

A novel filter scheme, called the SA filter, has been presented to allow precise real-time modeling of the absorption effect due to air, and a method has been described to derive coefficients a and b from published data. A cascade of two SA filters, with different coefficients, enables both a realistic simulation of air absorption effects at low temperatures, and fine tuning of the frequency response roll-off, with limited computing resource requirements (a relevant aspect for multichannel implementations). The described method to calculate coefficient b from the variable distance of a virtual source, by means of a simple linear control law, makes the SA filter an ideal algorithm for realistic real-time simulation, as filter coefficients derivation do not require iterative methods but can be computed at full speed, ensuring a filtering effect without glitches or discontinuities on audio data.

	RH = 10%		RH = 20%		RH = 40%		RH = 60%		RH = 80%		RH = 100%	
	***a*1**	***a*2**	***a*1**	***a*2**	***a*1**	***a*2**	***a*1**	***a*2**	***a*1**	***a*2**	***a*1**	***a*2**
	0,01	0,98	0,017	0,98	0,04	0,82	0,07	0,87	0,11	0,89	0,15	0,83
	***b*1**	***b*2**	***b*1**	***b*2**	***b*1**	***b*2**	***b*1**	***b*2**	***b*1**	***b*2**	***b*1**	***b*2**
10m	0,0017	0,022	0,0035	0,022	0,01	0,015	0,0148	0,02	0,023	0,02	0,03	0,025
20m	0,0036	0,044	0,007	0,044	0,018	0,03	0,0296	0,02	0,046	0,02	0,06	0,045
30m	0,0052	0,065	0,0105	0,066	0,026	0,05	0,0444	0,06	0,069	0,06	0,091	0,065
40m	0,0070	0,087	0,014	0,089	0,033	0,07	0,0592	0,08	0,092	0,08	0,121	0,08
50m	0,0085	0,109	0,0175	0,115	0,042	0,08	0,0740	0,1	0,115	0,1	0,151	0,1
60m	0,0105	0,135	0,021	0,137	0,051	0,085	0,0888	0,12	0,136	0,12	0,18	0,1152
70m	0,012	0,16	0,0245	0,162	0,06	0,115	0,1036	0,14	0,155	0,14	0,21	0,13

Table 2: List of the coefficients $a1$, $a2$, $b1$, $b2$ calculated for T = -20°C at varying of distance and relative humidity.

	RH = 10%		RH = 20%		RH = 40%		RH = 60%		RH = 80%		RH = 100%	
	***a*1**	***a*2**	***a*1**	***a*2**	***a*1**	***a*2**	***a*1**	***a*2**	***a*1**	***a*2**	***a*1**	***a*2**
	0,0503	0,849	0,1395	0,8455	0,28	0,65	0,43	0,6	0,5	0,63	0,6	0,63
	***b*1**	***b*2**	***b*1**	***b*2**	***b*1**	***b*2**	***b*1**	***b*2**	***b*1**	***b*2**	***b*1**	***b*2**
10m	0,0168	0,02	0,045	0,025	0,07	0,08	0,04	0,15	0,01	0,18	0,01	0,16
20m	0,034	0,02	0,095	0,043	0,14	0,15	0,13	0,22	0,05	0,32	0,012	0,31
30m	0,052	0,06	0,136	0,068	0,215	0,2	0,25	0,25	0,09	0,54	0,08	0,4
40m	0,069	0,08	0,182	0,085	0,3	0,22	0,36	0,3	0,2	0,75	0,14	0,64
50m	0,085	0,1	0,225	0,105	0,39	0,22	0,5	0,3	0,34	0,75	0,29	0,64
60m	0,102	0,12	0,266	0,126	0,56	0,05	0,65	0,3	0,5	0,7	0,49	0,69
70m	0,1182	0,14	0,31	0,1374	0,67	0,0	0,76	0,52	0,745	0,672	0,701	0,684

Table 3: List of the coefficients $a1$, $a2$, $b1$, $b2$ calculated for T = 0°C at varying of distance and relative humidity.

6. REFERENCES

[1] "*Acoustics - Attenuation of sound during propagation outdoors*" - ISO 9613-1, 1993

[2] Dennis A. Bohn, Rane Corporation, Everett, WA98201, USA, "*Environmental Effects on the Speed of Sound*", AES Convention 1987 October 16-19, New York

[3] J. Huopaniem, L. Savioja, M. Karjalanen, "*Modeling of Reflections and Air Absorption in Acoustical Spaces – A Digital Design Approach*", Proceedings of the 1997 IEEE ASSP Workshop on Applications of Signal Processing to Audio and Acoustics

[4] H.E. Bass, L.C. Sutherland, A.J. Zuckerwar, D.T. Blackstock,D.M. Hester "*Atmospheric absorption of sound: Further developments* ", J. Acoust. Soc. Am., Vol. 97, No. 1, January 1995

[5] Thomas D. Rossing, ed., "*Springer Handbook of Acoustics*", Springer, 2007

[6] Bass, H., and Bauer, H.-J., "*Atmospheric Absorption of Sound: Analytical Expressions*", J. Acoust. Soc. Am., Vol. 52, No. 3, 1972, pp. 821-825

[7] G. A Putland, "*Acoustical Properties of Air versus Temperature and Pressure*", JAES, vol. 42, no. 11, 1994, November

[8] Cyril M. Harris, "*Absorption of Sound in Air versus Humidity and Temperature*", NASA Contractor Report CR-647, 1967

[9] "*MARS Modules Reference Guide*", IRIS srl, Paliano, 1990

[10] Umberto Zanghieri, *"Study and realization of an apparatus for acquisition and analysis of guitar audio signals"*, Master Thesis, Università di Tor Vergata, Rome, October 1994